

NBER WORKING PAPER SERIES

PUBLIC AVOIDANCE AND THE EPIDEMIOLOGY OF NOVEL H1N1 INFLUENZA
A

Byung-Kwang Yoo
Megumi Kasajima
Jay Bhattacharya

Working Paper 15752
<http://www.nber.org/papers/w15752>

NATIONAL BUREAU OF ECONOMIC RESEARCH
1050 Massachusetts Avenue
Cambridge, MA 02138
February 2010

Prof. Yoo's work on this project is supported by National Institute of Health (1K25AI073915). Prof. Bhattacharya's work on this project is supported in part by the National Institute on Aging. We thank Peter G. Szilagyi, MD, MPH and Charles E. Phelps, PhD for their support in conception and Andrea Berry, MS for her data analysis and editing support. The views expressed herein are those of the authors and do not necessarily reflect the views of the National Bureau of Economic Research.

NBER working papers are circulated for discussion and comment purposes. They have not been peer-reviewed or been subject to the review by the NBER Board of Directors that accompanies official NBER publications.

© 2010 by Byung-Kwang Yoo, Megumi Kasajima, and Jay Bhattacharya. All rights reserved. Short sections of text, not to exceed two paragraphs, may be quoted without explicit permission provided that full credit, including © notice, is given to the source.

Public Avoidance and the Epidemiology of novel H1N1 Influenza A
Byung-Kwang Yoo, Megumi Kasajima, and Jay Bhattacharya
NBER Working Paper No. 15752
February 2010
JEL No. I1,I10

ABSTRACT

In June 2009, the World Health Organization declared that novel influenza A (nH1N1) had reached pandemic status worldwide. The response to the spread of this virus by the public and by the public health community was immediate and widespread. Among the responses included voluntary avoidance of public spaces, closure of schools, the ubiquitous placement of hand sanitizer, and the use of face masks in public places. Existing forecasting models of the epidemic spread of nH1N1, used by public health officials to aid in making many decisions including vaccination policy, ignore avoidance responses in the formal modeling. In this paper, we build a forecasting model of the nH1N1 epidemic that explicitly accounts for avoidance behavior. We use data from the U.S. summer and the Australian winter nH1N1 epidemic of 2009 to estimate the parameters of our model and forecast the course of the epidemic in the U.S. in 2010. We find that accounting for avoidance responses results in a better fitting forecasting model. We also find that in models with avoidance, the marginal return in terms of saved lives and reduced infection rates of an early vaccination campaign are higher.

Byung-Kwang Yoo
School of Medicine and Dentistry
601 Elmwood Ave, Box 644
Rochester, New York 14642
yoobk3@gmail.com

Megumi Kasajima
School of Medicine and Dentistry
601 Elmwood Ave, Box 644
Rochester, New York 14642
kasajimamegumi@gmail.com

Jay Bhattacharya
117 Encina Commons
Center for Primary Care
and Outcomes Research
Stanford University
Stanford, CA 94305-6019
and NBER
jay@stanford.edu

1. Introduction

In June 2009, the World Health Organization (WHO) declared a worldwide novel influenza A (nH1N1) pandemic alert (World Health Organization (WHO) 2009). As of December 2009, officials at the Centers for Disease Control estimated nearly 10,000 deaths due to nH1N1 infection between April and early December 2009 around the world (Centers for Disease Control and Prevention (CDC) 2009; World Health Organization (WHO) 2009). One unique feature of the novel influenza pandemic has been the widespread attention paid to it by the public. In Mexico, the U.S. and other countries, early reports about the novel influenza led to closure of schools, cancellation of public sporting events, and countless individual behavioral decisions regarding the extent to go out in public, e.g., during a school-closure period (Centers for Disease Control and Prevention (CDC) 2009). The decision to forego contact with other people is called an *avoidance response*. One implication of these sorts of public responses is that the illness attack rate and the reproduction rate (RR) of the virus (the number of secondary infected cases per primary infected case) are lower than they otherwise would be in the absence of an avoidance response.¹

Despite the importance of a public avoidance response on the illness attack rate and the RR of the virus, existing forecasting models of the novel influenza pandemic do not account for it (Boelle et al. 2009; Fraser et al. 2009; Yang et al. 2009).

Economists have found avoidance response to be important in other infectious disease contexts, including seasonal influenza vaccination (Li et al. 2004; Yoo and Frick 2005; Yoo et al. 2009) and measles vaccination (Philipson 1996). Researchers have found that higher disease prevalence motivates people to undertake activities that subsequently reduce the extent of an

¹ The RR plays a key role in models forecasting the extent of an epidemic. For example, if $RR < 1$ the outbreak will eventually die out.

epidemic. The logic runs in the opposite direction as well—a decreasing disease prevalence may lead to a reduction in preventive behaviors that makes it difficult to eradicate a preventable infectious disease even if an effective vaccine is available (Philipson 2000).

Our aim here is to develop a better forecasting model for the nH1N1 pandemic path from April 2009 to September 2010 by incorporating this concept of avoidance response, in comparison with models that do not include this concept. A secondary aim is to forecast the benefit of vaccination programs (available from October 2010) in changing the U.S. nH1N1 pandemic path, as well as its final size, using the most recently available information about the pandemic, e.g., the past winter pandemic in Australia, and the newly developed nH1N1 vaccines.

2. A Model of Avoidance

The main tool we use in our analysis is a three-compartment differential equation model, known in epidemiology as a “susceptible-infected-recovered” (SIR) model (Rvachev and Longini 1985). In this model, people transition between three mutually exclusive health states—susceptible to nH1N1 influenza, infected, and recovered (and hence immune). Let N_t be the total population in a given state as of July 1, 2008 (US Census Bureau)—we conduct a separate estimation for each state in the U.S. N_t is the sum of four terms: S_t (the number of susceptible people), I_t (the number of infected people), R_t (the number of recovered, and hence immune, people), and total deaths.² The model these compartments follow the following equations of motion over time:

$$(1) \quad \frac{dS_t}{dt} = -\frac{\beta_t S_t I_t}{N_t}$$

² For simplicity, we assume N_t is constant for all t . This is a reasonable assumption because the population size of each state is orders of magnitude larger than the number of people infected with nH1N1.

$$(2) \quad \frac{dI_t}{dt} = \frac{\beta_t S_t I_t}{N_t} - (\gamma + \alpha) I_t$$

$$(3) \quad \frac{dR_t}{dt} = \gamma I_t$$

The three parameters α , β_t , and γ denote the case fatality rate, the attack rate and the recovery rate, respectively. The first term of $\frac{dI_t}{dt}$ represents newly infected people moving from compartment S to I at time t ; γI_t represents those who recover from nH1N1 infection and hence move from compartment I to R at time t ; and finally, αI_t represents those who die from infection at time t .

The standard SIR-model assumes that the illness attack rate, which is the rate at which susceptible become infected, depends upon two factors. The first is the rate of transmission from a single contact between an infected and susceptible individual. The second is the frequency of such contact among individuals, which varies across people of different age, family size, and other factors (Coulombier and Giesecke 2009).

We modify this standard model to incorporate avoidance response—that is, the idea that the frequency of contact among individuals will itself depend on the prevalence of the disease in the population. Unlike the standard SIR-model, in our model the attack rate changes over time as disease prevalence changes. We assume attack rate to be the product of three factors: a constant baseline attack rate that represents a “biological” transmission rate; a baseline contact frequency which differs among subgroups; and avoidance response parameters which are influenced by the prevalence rate of the disease. Because the attack rate in our model changes over time, so does the reproductive rate of the virus. The appendix section provides more details. There, we also

describe how we estimate the parameters of the model and how we modify the model to account for vaccination against nH1N1 infection.

3. Methods

Our empirical analysis consists of three steps. First, we specify and estimate a model of the nH1N1 flu epidemic along the lines of the model described in the previous section. The Appendix provides details on our primary data source—laboratory confirmed daily reports on nH1N1 cases—and on our estimation procedure. We estimate versions of the model that account for avoidance behavior as well as versions of the model that do not. We also estimate separate versions of the model using data from Australia. Second, we use our models to forecast the baseline U.S. pandemic path (without vaccination) between April 2009 to September 2010. Our preferred forecast accounts for avoidance response. In these forecasts, we assume that severity of the epidemic mimics the severity experienced in Australia between May 2009 and September 2009 during its winter flu season. Finally, we characterize the benefit of vaccination programs (available since October 2010) in changing the U.S. H1N1 pandemic path.

3.1 Testing validity of avoidance response model

Our primary data sources consist of daily counts of laboratory confirmed reports from the U.S. (at the state level) between April 23, 2009 to July 17, 2009 (Centers for Disease Control and Prevention (CDC) 2009) and from Australia between May 9, 2009 to September 18, 2009 (also at the state and province—hereafter jurisdiction—level) (Australian Government Department of Health and Ageing 2009). These cases represent only a small fraction of all nH1N1 cases as the vast majority of H1N1 cases are not laboratory confirmed. In our models we assume a case

detection rate of 5%; that is, the CDC's report of over 40,000 laboratory confirmed cases over the observation period implies that there were 1 million infected cases in the U.S. (Centers for Disease Control and Prevention (CDC) 2009). This assumption is consistent with CDC guidelines as well as U.S. experience during previous flu epidemics. We estimate versions of this model in which we assume values of up to 10% for the case detection rate.

Our model also requires information on how long each infection lasted, which is not available in the CDC data. Based on data from previous flu epidemics, we assume a distribution of infection length with a mean of 4.1 days. For each case in the CDC data, we draw a random infection length from this distribution. We then aggregate over individual cases back to the day and state level to derive a panel of nH1N1 cases for each state in the U.S. over 86 days. We derive, using similar methods, a similar secondary dataset for Australia.

We assume that fatality rate among nH1N1 cases was 1% with a range of 0.5%-1.2%. We base this assumption on the observed confirmed-case fatality rate in the U.S. and Australia (Australian Government Department of Health and Ageing 2009; Centers for Disease Control and Prevention (CDC) 2009) and a recent study (President's Council of Advisors on Science and Technology 2009).

We estimate several different versions of our SIR model using a generalized least estimator. As we have said, we estimate a version of the model that permits an avoidance response. In addition, we estimate a version of our model in which we impose that there be no avoidance response. Our purpose is to compare the predictions of these two versions of the model against the actual path of the epidemic after September 2009. For both of these versions, we conduct obtain separate estimates for two groups of states with higher and lower epidemic levels. The higher epidemic level group includes the ten states— California, Connecticut, Florida, Illinois,

Massachusetts, New Jersey, New York, Pennsylvania, Texas, and Wisconsin—that had at least 1,000 confirmed cases per state. Together these states consist of 70% of the national confirmed cases in total as of July 3, 2009 (Centers for Disease Control and Prevention (CDC) 2009). We also estimate a separate version of the model with the Australian data.

Since the infection length is randomly drawn in the underlying data, we conduct 200 iterations of our estimation procedure. In each iteration, we draw a new infection length realization for the entire data set. Using the panel dataset produced in each iteration of the microsimulation model, we generate 200 different estimates of the parameters of our SIR model, once for each iteration.

3.2 Forecasting the baseline U.S. pandemic path without vaccination

Using our SIR model and the parameters derived from the estimation procedure, we calculate a predicted path of the U.S. pandemic between April 23, 2009 and July 17, 2009. We compare these predictions against the actual path of the epidemic over that period. We similarly calculate a predicted path of the Australian epidemic between May 9, 2009 and September 18, 2009 and compare against the actual path. Since the vaccine against nH1N1 was not available at all during this time, the estimates we produce in this section ignore any possible benefit from a vaccine in reducing the spread of infection.

We use our model to forecast the path of the U.S. epidemic after September 1, 2009, which we call the “U.S. winter.” In these forecasts, we use the illness severity parameters from the Australian version of the SIR model. There are at least two reasons why using the Australian winter pandemic parameters to forecast the U.S. winter pandemic is justified. First, the reproduction rate of the flu virus, including nH1N1 varies with the ambient temperature, and is

higher in the winter than it is in the summer. Thus, the Australian experience during the winter provides a better guide for the U.S. winter than does the U.S. summer experience. Second, the Australian population is among all nations in the Southern Hemisphere, most similar to the U.S. in terms of its health status and social-demographic characteristics at the national level. In addition, the information released to the general public about the pandemic in both countries by their respective governments and by the mass media is similar. The average of the mortality rate due to pneumonia and influenza in the past three years, prior to the nH1N1 pandemic, was similar: 0.020% in the U.S. (Centers for Disease Control and Prevention (CDC)), and 0.013% in Australia (Australian Bureau of Statistics 2009; Australian Bureau of Statistics 2009).

3.3 Characterizing the benefits of nH1N1 vaccination

Our analysis up to now has been predicated on the assumption that there is no effective vaccine available against nH1N1 infection. As an extension to our work, we modify our procedure to take account of the fact that a vaccine did actually become available in the U.S. in October, 2009. The details of this modification to our SIR model to account for vaccination are described in detail in the Appendix. Our modified SIR model reflects the most recent information available to us at the time of our writing: in October 1-7 there were 1 million doses per day of the vaccine, in October 8-14, 6 million doses per day, in October 15- December 2, 3 million doses per day. In total, there were 196 million doses available (McNeil 2009; McNeil 2009).

In this version of our model, we assume that the vaccine uptake rate ranges between 50% and 90%. At 50%, we effectively assume that everyday 0.5 million doses (out of 1 million doses available) were delivered and effective, and that the remaining 0.5 million doses were left unused by the end of a simulation period. For simplicity and because there are no on-point data

currently available, we assumed vaccine doses to be distributed equally across the all U.S. subpopulations. A 50% uptake rate is plausible because often a large number of doses remain unused even during past usual influenza seasons with vaccine supply problems (Orenstein and Schaffner 2008).

4. Results

4.1. *Testing the validity of avoidance response models*

Figure 1 plots the cumulative path of confirmed nH1N1 infected cases in the U.S. between April 23 and July 17, 2009 as represented in the CDC data and assuming a 5% case detection rate. Figure 1 also shows the epidemic paths forecasted by our primary model (solid line) accounting for avoidance response between April 23 and August 31, 2009. It also plots the 2.5 and 97.5 percentile paths (based on case rates on the last day) among 200 iterations of that model, indicated by dotted lines. Both models produce estimates with a narrow interval between the 2.5 and 97.5 percentile paths. Finally, Figure 1 plots the epidemic path implied by the version of the model in which there is no avoidance response. Evidently, not accounting for the avoidance response models produces a predicted epidemic path that does a poor job of fitting the actual data on cumulative infected cases over the observed period.

4.2. *Forecasting the baseline U.S. pandemic path without vaccination*

Figure 2 indicates our forecasts of the the path of the nH1N1 pandemic in the U.S. up to September 2010 (extending the time period shown in Figure 1) in the absence of a vaccination campaign. We plot three different forecasts. The first assumes that there is no avoidance response, while the second and third forecasts incorporate an avoidance response. The second

model is exactly the one we described in section 4.1 above. The third model incorporates a renewed upsurge in nH1N1 infections in the fall of 2009, using the “winter” parameters derived from the Australian data microsimulation.

The model which assumes no avoidance response predicts that the epidemic should have died out completely by August 31, 2009 with 61.1% of the population infected at some point during the pandemic. The second model, which incorporates avoidance response forecasts that the epidemic will continue throughout the simulation period of 500 days, with about 46.2% of the population infected by September 2010. In this avoidance response model, the reproduction rate (*RR*) of the virus fluctuates around 1.1 in the 10 states with high incidence rate and around 0.9 in the 40 states with low incidence.

In third model we use to forecast the pandemic path , the two key factors are the onset timing of the second epidemic upsurge and the severity of “winter” parameters derived from the Australian data microsimulation. In this Australian microsimulation model, we found a median illness attack rates that ranged between 0.23 and 0.74 (with an average rate of 0.68) among eight jurisdictions. Our baseline forecasts assume an attack rate of 0.68 to forecast a U.S. winter epidemic. In our forecasts, on the first onset day of the second epidemic upsurge, we replaced the measured attack rate in each U.S. state with the Australian number. Prior to the onset of the second upsurge (either September 1 or October 1), the mean illness attack rates was 0.29 in the highest incidence states and 0.22 in the lowest incidence states. This model (also shown in Figure 2) forecasts that the epidemic will die out in January 2010 with 40% of the population ultimately infected.

The forecasts of the baseline U.S. pandemic path from April 23, 2009 to September 5, 2010 are summarized under seven alternative scenarios in Tables 1 and 2. Table 1 shows the

proportion of the population ultimately infected, total deaths from the epidemic, and the effect of a vaccination campaign on these measures. Table 2 shows the forecasted peak pandemic prevalence rate and the peak date, as well as the effect of a vaccination campaign on these measures. The seven scenarios differ with regard to assumptions about the presence and timing of a second epidemic upsurge (indicated in column 1) and about whether there is a vaccination campaign. In all seven scenarios we assume there is an avoidance response. In column 2, we indicate our assumption about whether a vaccination campaign takes place, as well as our assumption about vaccine effectiveness in those scenarios where there is a campaign. Column 3 shows our assumption about the vaccination uptake rate (either 50% or 90%) if there is a campaign. Columns 4 and 5 in Table 1 show forecasted total pandemic impacts measured by the cumulative infected population over the course of the epidemic and total deaths, while columns 4-5 in Table 2 indicate the forecasted pandemic peak measured by the prevalence rate and the peak date. Columns 6 and 7 in each table show the forecasted effect of vaccination on epidemic paths and impacts.

Our models with avoidance response have the following bottom line implication for the path of the epidemic in the U.S. (shown in Table 1). If there is a second upsurge, we forecast that between 33.9% and 57.7% of the population will ultimately be infected. Without a second upsurge (scenario 7), we forecast 46.2% will ultimately be infected. We forecast that the peak of the upsurge occurs within three weeks of onset with a maximum prevalence ranging between 5.5% and 7.5% if the second upsurge occurs (Table 2). Without a second upsurge, we forecast a peak to occur as late as mid-February with a much lower maximum prevalence rate of 1%.

4.3. *Forecasting the benefits of a vaccination campaign in the U.S.*

Since there is an effective vaccine for nH1N1 infection which has been developed (Hancock et al. 2009) and widely distributed despite early shortages (McNeil 2009; McNeil 2009), it is important to account for it in our forecasts. Figure 3 presents our estimates that take this vaccination campaign into account. Our worst case scenarios assume that the vaccine is 50% vaccine effective and that 50% of the population ultimately uptake the vaccine. Our forecasts when the vaccine is available are sensitive to the timing of the second surge in nH1N1 infections. A delayed second upsurge (particularly the October onset) leads to a lower proportion of the population ultimately infected because the immune protection conferred by the vaccine (which typically takes up to 9 days) has more time to take hold. For instance, if there is a second upsurge, we forecast that 57.2% of the population will ultimately be infected if the second surge starts in September, 36.3% if the surge starts in October (also in columns 4 in Table 1). Our conservative scenarios with the vaccine predict and a 1% confirmed-case fatality rate imply that there will be between 55,100 and 86,900 total deaths in the U.S. due to nH1N1 infection.

Figures 5 and 6 present the four scenarios (from the 7 scenarios presented in Tables 1 and 2) that we believe are most likely to occur.³ . In two scenarios we assume a second upsurge starting on September 1, 2009, and in the other two scenarios we assume a second upsurge starting on October 1, 2009. All four scenarios assume 50% vaccination effectiveness. These correspond to scenarios 3-7 in Tables 1 and 2.

Figure 4 indicates the forecasted benefits from vaccination in terms of reductions in proportion of the population ultimately infected. Increasing the vaccination uptake rate from 50% to the maximum 90% (of the 196 million doses available) reduces the final size of the epidemic from 57.2% to 56.8% of the population in the scenarios with an September onset of the

³ The reasons for choosing these scenarios are detailed in the Discussion section.

second upsurge, and from 36.3% to 33.9% in those scenarios with the October onset second upsurge (also in Columns 4 and 6 in Table 1).

Figure 5 shows the benefit of the vaccination campaign in terms of reducing the peak levels of the epidemic. We plot the same four scenarios that we plot in Figure 4. If a second upsurge begins on October 1, a vaccination program starting October 1 with the 90% uptake rate and 50% effectiveness will reduce the peak prevalence only slightly from 5.56% to 5.50% and move peak timing by one day earlier (also in Columns 4-7 in Table 2). When a second upsurge begins on September 1, vaccination won't make any change due to its availability after October. If there is a severe second surge starting in November 1, this same vaccination program will reduce the peak prevalence from 5.35% to 3.5% and delay the peak date by one day.

5. Discussion

In this section, we discuss our view on which of our forecasted paths are most likely to occur. While this exercise is necessarily speculative, we include it because it helps make clear which of the various moving parts of our model are most important in reality. Figures 5 and 6 show the epidemic paths from the versions of the model that we believe to be most accurate. The forecasted paths in those figures account for demonstrated vaccine efficacy (Hancock et al. 2009), reported vaccine availability (McNeil 2009; McNeil 2009), and the U.S. pandemic situation as of October 17, 2009 (Centers for Disease Control and Prevention (CDC) 2009).

In the U.S., the second pandemic upsurge started in 12 states in early September 2009 and spread to 46 states by mid-October (Centers for Disease Control and Prevention (CDC) 2009). Therefore, the scenario 7 in Table 1, which forecast no second upsurge, will not occur. We include it partly because there may be other flu variant epidemics in the future where such

forecasts are appropriate, and partly because it is a good reference in comparison with the non-response model in Figure 2 that died out prior a second upsurge in fall 2009.

The number of people infected by the nH1N1 virus has been increasing since early September 2009, exceeding the levels of regular seasonal influenza and the first H1N1 upsurge in May 2009 in the U.S. The number of infected individuals has yet to reach a peak as of October 17, 2009, based upon the percentage of visits for influenza-like illness (ILI) at the national level (Centers for Disease Control and Prevention (CDC) 2009). Thus, for the national level forecasts, the scenarios forecasting an epidemic peak timing prior to mid-October (such as those which assume no avoidance behavior) are not appropriate.

Based on this reasoning, we identify those scenarios in which effective vaccines are available starting in October and in which a second upsurge occurs as most appropriate (Scenarios 1-6 in Tables 1 and 2). Among these scenarios, the forecasts imply: (1) between 33.9% and 57.7% of the population ultimately infected with nH1N1 flu; (2) between 51,600 and 87,700 as a result of the nH1N1 flu; (3) a peak prevalence between 5.50% and 7.46% of the population; and (4) a peak level of the epidemic occurring between September 21 and October 19, 2009. The forecasted ranges of vaccination benefits were as follows: (1) a reduction in the total population ultimately infected between 0.8% and 6.2% of the population; (2) a reduction in total deaths due to the vaccine of between 1,300 and 9,500 people; (3) a reduction in the peak prevalence of the epidemic of between 0.00% (that is, less than 0.00 and 0.16% of the population; and (4) a change in peak timing of the epidemic of only 1 day.

Our forecasts from the scenarios that we identify as most appropriate are qualitatively similar to other recent forecasts of the nH1N1 epidemic. Yang and colleagues estimated the total infected cases in the total U.S. population with three levels of pandemic transmissibility: (i) 21-

31% (low transmissibility), (ii) 32-39% (moderate) and (iii) 40-49% (high) (Yang et al. 2009).

The President's Council of Advisors on Science and Technology published a scenario in which 30% to 50% of the population is ultimately infected and there are between 30,000 and 90,000 deaths (President's Council of Advisors on Science and Technology 2009). These death estimates are smaller than earlier estimates published by the U.S. Department of Health and Human Services, which predicted 90 million infected cases (30% of the U.S. population) and between 209,000 and 1,903,000 deaths (the latter case assumes that the nH1N1 has characteristics similar to the 1918flu virus) (United States Department of Health and Human Services (DHHS) 2009).

The forecasted range of deaths (51,600- 87,700) in our likely scenarios is likely to be comparable or greater than all-associated deaths due to seasonal influenza (36,200 with a range of 8,097-51,203) (Thompson et al. 2003) and largely overlaps with the recent government report (30,000-90,000) (President's Council of Advisors on Science and Technology 2009) mentioned earlier.

Deaths due to pandemic nH1N1 are likely to add to, rather substitute for, seasonal influenza deaths because the two flu strains affect different populations. nH1N1 flu is more likely than seasonal flu to kill younger people, while around 90% of the influenza-related deaths in the U.S. occur among the elderly (Thompson et al. 2003).

Our estimate of the benefits of vaccination are difficult to compare directly with past studies because these studies use different assumptions about vaccination policy (for example, some studies assume that two vaccine doses for adults as well as children), priorities in target subpopulations, and in vaccine availability (Flahault et al. 2009; Yang et al. 2009). The assumptions we make on these points reflect actual vaccine availability and actual vaccination policy. Yang et al. (2009) estimate only a small benefit from universal vaccination with a 30

day delay—a reduction of in the ultimate proportion of the population infected between 10% and 15% if there is a moderate pandemic, and less than 7% if there is a severe pandemic.

6. Conclusion

In our view, the two most important contributions of this paper are: (1) to highlight the importance of accounting for avoidance response in SIR models of infectious disease spread, when such a response is possible, and (2) to show that vaccination campaigns are most effective if they take place before an epidemic has spread. While these are not new insights (Philipson 2000; Yoo et al. 2009), they have not been widely understood in the applied literature on disease epidemics and to our knowledge have not been applied in the case of the nH1N1 flu epidemic at all. These two results highlight the difficulty that public health officials face in managing an infectious disease like the nH1N1 flu. At the time when vaccination would be most effective, demand for the vaccine is lowest because the prevalence of the disease is low. These results also emphasize the importance of avoiding early shortages of vaccines during a flu epidemic.

We show that it is possible to fit SIR models that take into account of the population's avoidance response to an epidemic using readily available data. Accounting for this response involves a simple modification to a standard SIR model, but results in a substantially better fit to the data. In the case of nH1N1 flu, accounting for avoidance makes particular sense since the spread of the flu has led the closure of schools and other costly responses aimed at decreasing the spread of infection. More accurate pandemic path forecast regarding the peak timing and the peak level of an epidemic is also particularly useful in aiding public health officials to allocate limited resources in a setting where vaccine availability is limited.

We find evidence of the importance of accounting for an avoidance response in both the U.S. and in Australia. Our finding that baseline pandemic path and proportion ultimately infected are lower because of a robust avoidance response is consistent with common sense, as well as the literature on economic epidemiology. For instance, Yoo et al. (2009) found a robust avoidance response in the context of the seasonal flu among a nationally-representative elderly people in the U.S. (Yoo et al. 2009). If the models of other studies (Boelle et al. 2009; Fraser et al. 2009; President's Council of Advisors on Science and Technology 2009; Yang et al. 2009) also account for avoidance response, their forecasts of ultimate epidemic size would likely decrease as they did in our forecasts.

One limitation of our study is that we rely on case report data from the CDC which is certainly measured with error (Centers for Disease Control and Prevention (CDC) 2009). These data are known to face biases due to under-reporting and delayed-reporting. Though it is impossible to know how extensive. To address this limitation, we vary our assumed detection rate over a considerable range in our sensitivity analysis. These sensitivity analyses show that several of our most important results (such as the shape of the epidemic paths and our estimates on confirmed cases and deaths) are only modestly influenced by such measurement errors.

A second limitation is that our models do not explicitly account for the effect of antiviral medication in reducing the length of infection. In a sense, we do account for the use of drugs such as Tamiflu in our forecasts because we rely on actual case reports of nH1N1 data. These data reflect the effects of antivirals as they are actually used in the population. Unless the pattern of use of antiviral medications has changes between September 2009 and September 2010, which appears less likely according a recent CDC report (Centers for Disease Control and Prevention

(CDC) 2009), our forecasts of pandemic path and vaccination benefits are unlikely to be affected by this limitation.

A third limitation is that we do not calculate separate forecasts of the effect of the epidemic on heterogeneous groups in the population. This is an important omission because, as we have noted, the nH1N1 flu virus affects people of different ages differently. As the next step in this research agenda, we are planning to address this lacuna by incorporating avoidance response into agent-based models, which explicitly account for heterogeneous characteristics across subpopulations (Longini et al. 2004; Ferguson et al. 2006).

In part because of avoidance behavior (including the closing of schools and the avoidance by individuals of public places at the peak of the epidemic), we expect that the nH1N1 influenza pandemic this year to be relatively mild in the U.S. when compared with past pandemics but likely to be comparable to or more severe than the typical seasonal influenza epidemic. To the extent that people continue to avoid public places throughout the year due to the nH1N1 epidemic, the seasonal flu epidemic this year will also be less severe than it might have been. However, the fact that avoidance in the face of an epidemic is an important phenomenon makes the early availability of vaccines more important not less. We argue these lessons ought to be incorporated into forecasts of future flu epidemics of all sorts. More accurate and more useful forecasts will result and better enable public health officials to make good decisions about the allocation of limited funds, anti-virals, vaccines, and other resources such as quarantines and school and public event closures to mitigate the impact of future pandemics.

Appendix

Our aim in this paper is to develop and estimate a model of the nH1N1 epidemic that takes account of the avoidance response to the spread of the virus. We rely on the experience of the U.S. and Australia in the early stages of the epidemic as our primary data sources. We estimate the parameters of our model using these data and then forecast the implications of our model for the future of the epidemic. In this appendix, we describe our empirical work in some detail.

A.1. Inferring the Number of Susceptible, Infected, and Recovered from CDC Data

We construct a microsimulation model of the nH1N1 epidemic with the aim of estimating the attack rate of the nH1N1 influenza on each of the 86 days between April 23, 2009 and July 17, 2009 of our U.S. data. We forecast the course of the epidemic separately for every state in the U.S. This section explains the microsimulation procedures to estimate the numbers of infectives (I_t), recovered (R_t), susceptibles (S_t), and the state-specific daily attack rate (β_t). At the end of the section, we go through a hypothetical example of our microsimulation exercise to illustrate how we estimate the number of infectious cases (I_t).

We start with our procedure to estimate the number of infectious cases (I_t). Our primary data source is the Centers for Disease Control (CDC) which reports the cumulative daily number of state-specific laboratory confirmed cases of nH1N1 starting on April 23, 2009. The CDC data correspond to $\frac{dI_t}{dt}$ in our notation. However, since not every case of nH1N1 is laboratory confirmed, we need an assumption about the detection rate. In our base case, we assume a detection rate of 5%, which implies that the CDC measures only one in 20 of the actual cases

(Centers for Disease Control and Prevention (CDC) 2009). In sensitivity analyses, we assume a 10% detection rate, which cuts our forecast in half.

The CDC data does not indicate the date when an infected individual exited the infective compartment, so we need a credible assumption to infer the exit date (i.e., length of stay in the infective compartment, or the infectious period) for each case who contracts nH1N1 disease. Following past studies (Elveback et al. 1976; Longini et al. 2005), to each person in the CDC database we randomly assign the infectious period (τ) as 3 days (with the probability of 0.3), 4 days (0.4), 5 days (0.2) or 6 days (0.1), which implies that the mean length of infection period is 4.1 days. We additionally assume that the infectious period distributions are the same for individuals who recover and individuals who die from nH1N1 infection. Together, these assumptions imply that $(\alpha + \gamma)^{-1} = 4.1$.⁴ We adopt these periods with probabilities, partly because data on this parameter for nH1N1 are not available and partly because these values are within the range of the CDC's interim guideline for nH1N1 influenza (Centers for Disease Control and Prevention (CDC) 2009).

Let $\{\tau = k \mid k = 3, \dots, 6\}$ represent the set of infected patients in the CDC database to whom we randomly assign to an infectious period of k days. Under our assumptions, the total number of infected individuals today equals the sum over all the patients who transitioned into the infected compartment over the past six days. Thus, the total number of infected people on day t is given by:

$$(A1) \quad I_t = \left(\sum_{k=0}^2 \frac{dI_{t-k}}{dt} \right)_{\tau=3} + \left(\sum_{k=0}^3 \frac{dI_{t-k}}{dt} \right)_{\tau=4} + \left(\sum_{k=0}^4 \frac{dI_{t-k}}{dt} \right)_{\tau=5} + \left(\sum_{k=0}^5 \frac{dI_{t-k}}{dt} \right)_{\tau=6}$$

⁴ Recall that α is the case mortality rate and γ is the case recovery rate.

For simplicity, we assume that newly infected individuals had a laboratory test and were diagnosed on the first day of their infection. Therefore, if there was a one-week time-lag between the beginning of the infectious period and the laboratory test diagnosis among all infected cases, our estimated epidemic paths will reflect an epidemic one week prior. We experimented with altering our assumptions about the length of this time-lag; these experiments led us to conclude that this assumption has little effect on the time path and magnitude of the forecasted epidemic.

Next, we describe our procedure for estimating the number of recovered (R_t) and susceptible (S_t) individuals. Among those exiting the infective compartment, we assumed that the death rate was a constant 1%. We base our assumption on case reports of nH1N1 infection (Australian Government Department of Health and Ageing 2009; Centers for Disease Control and Prevention (CDC) 2009; President's Council of Advisors on Science and Technology 2009). We calculate R_t simply as the cumulative number of survivors among the infected as below.

$$(A2) \quad R_t = \int_0^t I_x dx$$

Our calculation of S_t follows from the definition of N as the population size in any given state. N is the sum of four terms: total deaths due to novel influenza infection, S_t , I_t , and R_t . Therefore, the number of susceptible people is $S_t = N - I_t - R_t -$ (total deaths due to novel influenza infection at t).

Finally, we estimate the state-specific daily infection rate (β_t). Equation (2) from the main text, rearranged, implies the following:

$$(A3) \quad \beta_t = \frac{N_t \left[\frac{dI_t}{dt} + (\gamma + \alpha)I_t \right]}{S_t I_t}$$

Since we already either directly observe (in the case of $\frac{dI_t}{dt}$) or calculate all of the quantities on the right hand side of (A3), we have an estimate of β_t .

To characterize the uncertainty in this infectious period, we ran 200 iterations. In each iteration, we assigned each individual in the CDC database a new draw from the distribution of infective periods. This microsimulation data were generated to match with the real CDC-data in terms of the cumulative infectives on the final microsimulation day, July 17, 2009. For our base case of a 5% detection rate, we inflated the number of infected patients (I_t) (based on the confirmed cases) by 20 times by summing 20 iterations of the microsimulation by randomly choosing from the 200 iterations already created earlier. Similarly, for our sensitivity analysis of a 10% detection rate, we inflated I_t by 10 times.

A.2 Example of a microsimulation iteration

In this section, we illustrate our microsimulation procedure by walking through a single iteration in a single hypothetical state. For simplicity, we assume the CDC detects 100% of all nH1N1 cases in its data (in the actual simulation, we assume a 5% detection rate). Table A1 documents this example iteration. In our example, we suppose that one state reports two confirmed cases of nH1N1 infection on $t = 1$ but does not report any additional cases up to $t = 7$. On $t = 8$, the state reports a third case to the CDC. This is indicated on the first on the first row of Table A1.

For each case that arrives at $t = 1$, we draw a random number representing the number of days that each individual remains infected. For the first case, represented by the grey boxes on the second row of Table A1, we drew 3 days. For the second case, we drew 4 days. The total number of infected patients in the state on any particular day, equals the number of gray boxes in

any given column. Thus, the number of infected (I_t) individuals, shown on the fifth row of Table A1, is not constant. $I_1 = I_2 = I_3 = 2$; $I_4 = 1$; and $I_5 = I_6 = I_7 = 0$.

From the data on row 5, we calculate the number of individuals exiting the infective compartment at each t . These consist of those who recover or die from nH1N1 infection. In this hypothetical example, shown on row 6 of Table A1, one person leaves the infected state at $t = 4$ and another leaves at $t = 5$. Similarly, we can calculate the number of newly infected individuals—two people enter at $t = 1$ and then no one else enters after. This is shown on row 7 of Table A1. Finally, the change in the number of infected people, or $\frac{dI_t}{dt}$, is shown on row 8 of Table A1.

A.3. Estimation of baseline attack rate and avoidance response parameters

The procedure outlined in Section A.1 and illustrated in Section A.2 generates, for each state and at each time point, an enriched state-level data set from the original CDC data which includes the key time varying numbers we need to generate estimates of the baseline attack rate and the avoidance response parameters. In this section, we outline our methods for generating these latter quantities. Our primary technology involves estimating a generalized least squares (GLS) regression model from the panel of state data outlined in Section A.1 (for each iteration of the microsimulation model). At this point in the discussion, the variation across states becomes important since it is needed to identify our parameter estimates, so we subscript our variables and parameters with both i (representing each state) and t (representing each time point).

Our panel data includes the state-specific daily attack rate (β_{it}) and the number of infectious people (I_{it}) for each of 50 states and the 86 days that we observe in our data. We model β_{it} as follows:

$$(A4) \quad \beta_{it} = \beta_0 \exp(c_0 t - m_0 w(I_{it}))$$

where $w(I_{it})$ is a measure of the cumulative prevalence of nH1N1 disease over the previous seven days:

$$(A5) \quad w(I_{it}) = \ln \left(\sum_{T=t-8}^{t-1} I_{iT} \right)$$

We estimate β_0 , c_0 , and m_0 with generalized least squares (GLS) models by applying (A4) and (A5) to our panel data set. We perform the estimation separately for each of 200 iterations of the microsimulation models and also separately for each of the two groups classified based on the epidemic activity: one group with ten states with above median incidence and a second group of 40 states with below median incidence. The standard errors we report for the GLS model account for heteroskedasticity.

A.4. Forecasting and validation

Using our estimates from section A.3 and our microsimulation model—equations (1)-(3), (A4), and (A5)—we forecast the “baseline” path of the U.S. pandemic (without vaccination) between April 23, 2009 and July 17, 2010. Among the outputs of our forecast include the cumulative numbers of (both total and confirmed) infected cases, deaths, the reproduction rate (RR_t) of the virus, and the prevalence rate in the total population. We calculate the time-variant reproductive rate (RR_t) as the product of three terms: the attack rate, the proportion of susceptibles in the total population, and the duration in the infective compartment— $\beta_t \left(\frac{S_t}{N_t(\gamma + \alpha)} \right)$.

Since we run 200 sets of forecasts (one for each iteration of the microsimulation model) we can report representative sets of pandemic path based on the size of the epidemic. In Figures 1

and 2, we report paths that correspond to the median, and the upper and lower 95% percentiles of the final extent of the epidemic.

We also forecast versions of the model in which we assume that there is no avoidance response with $m_0 = 0$. Our purpose in these alternate forecasts is to determine whether forecasts produced using our primary avoidance response models fit better with the available data on the epidemic (that is, the confirmed cumulative infection rates up to July 17, 2009) than do models that ignore an avoidance response. The results from these comparisons are shown in Figures 1 and 2.

In the versions of the model that we report in the paper, we fit our models based on data spanning from May 7 to July 3, dropping the first and the last two weeks of the available data. Versions of model that do not drop these four weeks yield implausibly small epidemic impacts. Besides yielding more plausible results, there is another independent reason to drop these weeks. According to the CDC, data from these four weeks were subject to more serious underestimation of confirmed cases. This is because, in the early weeks there were only a limited number of laboratory test orders; in the later weeks, the surge in test orders were limited by the limited capacities of laboratory testing after the first pandemic upsurge in many states (Centers for Disease Control and Prevention (CDC) 2009). This was why CDC stopped collecting and releasing the detailed confirmed case numbers after July 17, 2009 (Centers for Disease Control and Prevention (CDC) 2009). Therefore, our paper presents results based on the U.S. data from May 7 to July 3.

In addition to our U.S. forecasts, we also perform an entirely parallel forecast using data from Australia. The methods we use for our Australian forecasts are exactly analogous to those we use in the U.S. forecasts. However, the Australian confirmed case data are available at the

jurisdiction-level (there are 8 jurisdictions in Australia) only up to July 19. After that date, there only data on confirmed cases are available are at the national level. So for the later period, we inferred jurisdiction based on our microsimulation results which allocated the daily newly national-level confirmed cases among eight jurisdictions. Our allocation rule assumes that the incidence ratios of the daily newly confirmed cases among eight jurisdictions are equal to those of the daily newly hospitalized cases among these jurisdictions.

A.5 Forecasting the benefits of vaccination in the U.S.

Our analyses shown in Figures 1-3 have been predicated on the assumption that there is no effective vaccine available against nH1N1 infection. As an extension to our work, we modify our procedure to take account of the fact that a vaccine did actually become available in the U.S. in October, 2009. Our modified SIR model reflects the most recent information: in October 1-7 there were 1 million doses per day of the vaccine, in October 8-14, 6 million doses per day, in October 15- December 2, 3 million doses per day. In total, there were 196 million doses available (McNeil 2009; McNeil 2009).

In this version of our model, we assume that the vaccine uptake rate ranges between 50% and 90%. At 50%, we effectively assume that everyday 0.5 million doses (out of 1 million doses available) were delivered and effective, and that the remaining 0.5 million doses were left unused by the end of a simulation period. For simplicity and because there are no on point data currently available, we assumed vaccine doses to be distributed equally across the all U.S. subpopulations. A 50% uptake rate is plausible because often a large number of doses remain unused even during past usual influenza seasons with vaccine supply problems (Orenstein and Schaffner 2008).

Let p be the uptake rate of the vaccine. We randomly select p percent of the individuals from the susceptible (S) and the recovered (R) compartments of the SIR model to receive the vaccine. We select people from R because in reality only a small proportion of the recovered population has a laboratory confirmed diagnosis of nH1N1. We assume, therefore, that all subjects in R wants to be vaccinated, which approximates the actual U.S. situation. (This assumption reduces the effectiveness of the vaccine because providing the vaccine to people in R does not contribute mitigating the pandemic. These individuals have presumably already gained natural immunity to nH1N1 infection which we assume to be 100% protective against H1N1 infection.)

Following the most recent vaccination guideline (Centers for Disease Control and Prevention (CDC) 2009), adults receive only one dose and children aged under 10 receive two doses separated by 28 days (second dose contained half the amount of the first dose). We account for this recommendation as well in our model.

We assume vaccination is 30%-70% effective in reducing infection, severe illness, and death due to novel influenza. We incorporated this assumption into our model as follows. Suppose vaccine effectiveness is 50%. In that case, only 50% of the vaccinated individuals transit directly from the susceptible (S) compartment directly into R without passing through the infected (I) compartment. The remaining 50% of these vaccinated individuals (with poor immune-response) remain in S despite vaccination. We assume that, these vaccinated with a poor immune-response were not vaccinated more than once, since individuals do not typically know their immune-response to a vaccine that requires a laboratory test.

The vaccine becomes protective roughly 9 days after it is administered. In the case of children under 10, it becomes effective only after the second dose (Centers for Disease Control and Prevention (CDC) 2009). We modeled this fact as follows: all of the vaccinated remain in

the susceptible compartment for 9 days after the vaccination date, except for children under 10 who remain in S for 37 days after the first vaccination.

Formally, let μ indicate vaccine uptake rate (ranging between 50% and 90%), let ρ indicate the proportion of population aged 10 or older, let θ indicate vaccine effectiveness (ranging between 30% and 70%), and let V_t indicate the total number of vaccine doses available on day t .

When we incorporate the assumptions about vaccination into our modified SIR model, equations (1)-(3) become:

$$(A6) \quad \frac{dS_t}{dt} = -\frac{\beta_t S_t I_t}{N_t} - \mu\rho\theta V_{t-9} \left(\frac{S_{t-9}}{S_{t-9} + R_{t-9}} \right) - \mu(1-\rho)\theta V_{t-37} \left(\frac{S_{t-37}}{S_{t-37} + R_{t-37}} \right)$$

$$(A7) \quad \frac{dI_t}{dt} = \frac{\beta_t S_t I_t}{N_t} - (\gamma + \alpha) I_t$$

$$(A8) \quad \frac{dR_t}{dt} = \gamma I_t + \mu\rho\theta V_{t-9} \left(\frac{S_{t-9}}{S_{t-9} + R_{t-9}} \right) + \mu(1-\rho)\theta V_{t-37} \left(\frac{S_{t-37}}{S_{t-37} + R_{t-37}} \right)$$

References

- Australian Bureau of Statistics. Australian Demographic Statistics. 2009. Retrieved September 25, 2009, from <http://www.abs.gov.au/AUSSTATS/abs@.nsf/second+level+view?ReadForm&prodno=3101.0&viewtitle=Australian%20Demographic%20Statistics~Mar%202009~Latest~22/09/2009&&tabname=Past%20Future%20Issues&prodno=3101.0&issue=Mar%202009&num=&view=&>.
- Australian Bureau of Statistics. Causes of Death, Australia. 2009. Retrieved September 25, 2009, from <http://www.abs.gov.au/AUSSTATS/abs@.nsf/second+level+view?ReadForm&prodno=3303.0&viewtitle=Causes%20of%20Death,%20Australia~2007~Latest~18/03/2009&&tabname=Past%20Future%20Issues&prodno=3303.0&issue=2007&num=&view=&>.
- Australian Government Department of Health and Ageing. Update Bulletins for Pandemic (H1N1) 2009. 2009. Retrieved September 25, 2009, from <http://www.healthemergency.gov.au/internet/healthemergency/publishing.nsf/Content/updates>.
- Boelle P Y et al. A preliminary estimation of the reproduction ratio for new influenza A(H1N1) from the outbreak in Mexico, March-April 2009. *Euro Surveill* 2009; 14; [Epub ahead of print].
- Centers for Disease Control and Prevention (CDC). H1N1 Flu (Swine Flu). 2009. H1N1 Flu Retrieved October 23, 2009, from <http://www.cdc.gov/h1n1flu/>.
- Centers for Disease Control and Prevention (CDC). National Vital Statistics Reports. 2009. Retrieved September 25, 2009, from <http://www.cdc.gov/nchs/products/nvsr.htm>.
- Centers for Disease Control and Prevention (CDC) Outbreak of swine-origin influenza A (H1N1) virus infection - Mexico, March-April 2009. *MMWR Morb Mortal Wkly Rep* 2009; 58; 467-470.
- Coulombier D and J Giesecke Why are Mexican data important? . *Euro Surveill* 2009; 14; [Epub ahead of print].
- Elveback L R et al. An influenza simulation model for immunization studies. *Am J Epidemiol* 1976; 103; 152-165.
- Ferguson N M et al. Strategies for mitigating an influenza pandemic. *Nature* 2006; 442; 448-452.
- Flahault A et al. Potential for a global dynamic of Influenza A (H1N1). *BMC Infect Dis* 2009; 9; [Epub ahead of print].
- Fraser C et al. Pandemic potential of a strain of influenza A (H1N1): early findings. *Science* 2009; 324; 1557-1561.
- Hancock K et al. Cross-Reactive Antibody Responses to the 2009 Pandemic H1N1 Influenza Virus. *N Engl J Med* 2009.
- Li Y C et al. Influenza and pneumococcal vaccination demand responses to changes in infectious disease mortality. *Health Serv Res* 2004; 39; 905-925.
- Longini I M, Jr. et al. Containing pandemic influenza with antiviral agents. *Am J Epidemiol* 2004; 159; 623-633.
- Longini I M, Jr. et al. Containing pandemic influenza at the source. *Science* 2005; 309; 1083-1087.
- McNeil D G Swine Flu Doses Will Be Double the Number Expected. *The New York Times*. New York, NY, The New York Times Company. September 25, 2009.

- McNeil D G Swine Flu Vaccine Will Be Too Late to Prevent Pandemic, Experts Say. The New York Times. New York, NY, The New York Times Company. September 15, 2009.
- Orenstein W A and W Schaffner Lessons learned: role of influenza vaccine production, distribution, supply, and demand--what it means for the provider. *Am J Med* 2008; 121; S22-27.
- Philipson T Private Vaccination and Public Health: An Empirical Examination for U.S. Measles. *The Journal of Human Resources* 1996; 31; 611-630.
- Philipson T (2000). Economic Epidemiology and Infectious Diseases. Handbook of Health Economic. A. J. Culyer and J. P. Newhouse. **1**: 1761-1799.
- President's Council of Advisors on Science and Technology (2009). Report to the President on U.S. Preparations for 2009-H1N1 Influenza. Executive Office of the President.
- Rvachev L A and I M Longini A Mathematical Model for the Global Spread of Influenza. *Mathematical Biosciences* 1985;3-22.
- Thompson W W et al. Mortality associated with influenza and respiratory syncytial virus in the United States. *JAMA* 2003; 289; 179-186.
- United States Department of Health and Human Services (DHHS). Pandemic Influenza. 2009. Retrieved April 28, 2009, from <http://www.dhhs.gov/nvpo/pandemics/>.
- US Census Bureau. United States 2008 Population Estimates. Retrieved April 28, 2009, from http://factfinder.census.gov/servlet/GCTTable?_bm=y&-geo_id=01000US&-box_head_nbr=GCT-T1&-ds_name=PEP_2008_EST&-lang=en&-format=US-40&-sse=on
- World Health Organization (WHO). Pandemic Phase 6. 2009. Retrieved June 12, 2009, from http://www.who.int/mediacentre/news/statements/2009/h1n1_pandemic_phase6_20090611/en/print.html.
- World Health Organization (WHO). Updates in confirmed cases in the world. 2009. Retrieved June 12, 2009, from http://www.who.int/csr/don/2009_06_12/en/index.html.
- Yang Y et al. The Transmissibility and Control of Pandemic Influenza A (H1N1) Virus. *Science* 2009; 2009/09/12; [Epub ahead of print].
- Yoo B K and K Frick Determinants of Influenza Vaccination Timing. *Health Economics* 2005; 14; 777-791.
- Yoo B K et al. Effects of ongoing epidemic on the annual influenza vaccination rate and vaccination timing among the Medicare elderly: 2000-2005. *American Journal of Public Health* 2009; 99; S383-S388.

Table 1. Forecasted novel H1N1 influenza pandemic total impacts and vaccination benefit measured by [final size and total deaths] in the United States from April 23, 2009 to September 5, 2010 (day 500)

scenario	Second upsurge†	Vaccination‡		Total impact		Vaccination benefit on total impact§	
	Onset of upsurge	Effective -ness	Uptake rate	Final size (Cumulative infected [%])	Total deaths	Reduction in cumulative infected	Reduction in total deaths
	[1]	[2]	[3]	[4]	[5]	[6]	[7]
1	Sep.1	n/a	n/a	57.7	87,686	n/a	n/a
2	Oct.1	n/a	n/a	40.1	61,030	n/a	n/a
3	Sep.1	50%	50%	57.2	86,922	0.50	763
4	Oct.1	50%	50%	36.3	55,144	3.87	5,886
5	Sep.1	50%	90%	56.8	86,407	0.84	1,279
6	Oct.1	50%	90%	33.9	51,555	6.23	9,475
7	None	n/a	n/a	46.2	70,186	n/a	n/a

†: Second upsurge: At the onset of a second upsurge, the illness attack rate increased to 0.68 in upsurge scenarios. These illness attack rates (0.68) were estimated with the past Australian “winter” data from April to September 2009, detailed in the text. Scenario 7 did not assume a second upsurge or use these Australian winter parameters.

‡: Vaccination effectiveness in reducing infection, severe illness and death due to novel influenza. Vaccine uptake rate among the available vaccine doses (October 1-7: 1 million doses per day; October 8-14: 6 million doses per day; October 15- December 2 (7 weeks): 3 million doses per day; 196 million doses in total)

§: Vaccination benefit compared to comparable scenarios (1-2) without vaccination.

Table 2. Forecasted H1N1 novel influenza pandemic peak and vaccination benefit measured by [peak prevalence rate and peak timing] in the United States from April 23, 2009 to September 5, 2010 (day 500)

scenario	Second upsurge †	Vaccination‡		Pandemic peak		Vaccination benefit on pandemic peak§	
	Onset timing	Effective -ness	Uptake rate	Prevalence [% total population]	Timing [Date]	Reduction in prevalence	Delayed in timing [days]
	[1]	[2]	[3]	[4]	[5]	[6]	[7]
1	Sep.1	n/a	n/a	7.46%	09/21/09	n/a	n/a
2	Oct.1	n/a	n/a	5.66%	10/19/09	n/a	n/a
3	Sep.1	50%	50%	7.46%	09/21/09	0.00%	0
4	Oct.1	50%	50%	5.56%	10/19/09	0.10%	0
5	Sep.1	50%	90%	7.46%	09/21/09	0.00%	0
6	Oct.1	50%	90%	5.50%	10/18/09	0.16%	1
7	None	n/a	n/a	1.00%	02/13/10	n/a	n/a

†: Second upsurge: At the onset of a second upsurge, the illness attack rate increased to 0.68 in upsurge scenarios. These illness attack rates (0.68) were estimated with the past Australian “winter” data from April to September 2009, detailed in the text. Scenario 7 did not assume a second upsurge or use these Australian winter parameters.

‡: Vaccination effectiveness in reducing infection, severe illness and death due to novel influenza. Vaccine uptake rate among the available vaccine doses (October 1-7: 1 million doses per day; October 8-14: 6 million doses per day; October 15- December 2 (7 weeks): 3 million doses per day; 196 million doses in total)

§: Vaccination benefit compared to comparable scenarios (1-2) without vaccination.

Table A1. Hypothetical example of microsimulation to estimate the number of infectives (I_t)

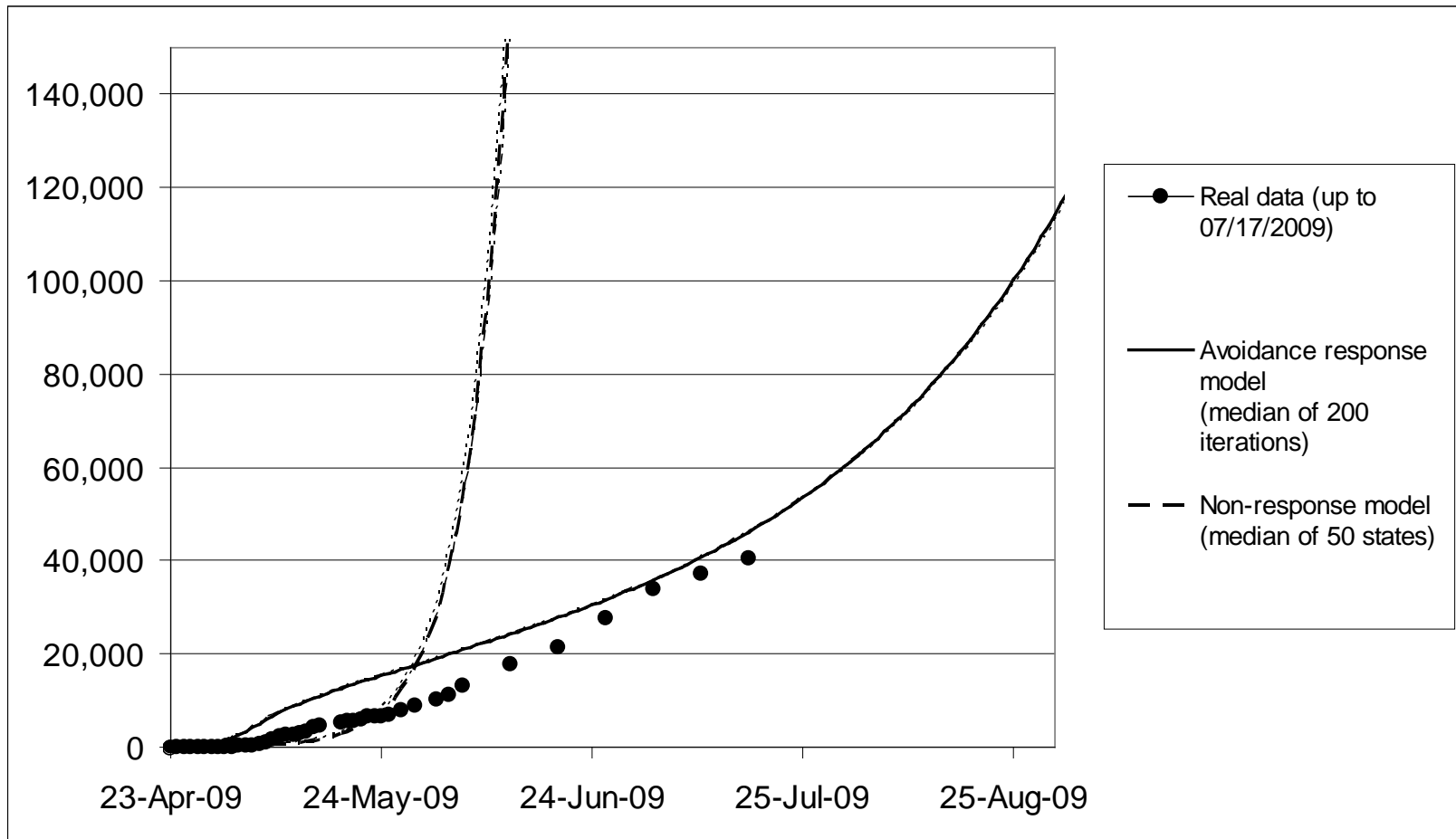
		$t=1$	$t=2$	$t=3$	$t=4$	$t=5$	$t=6$	$t=7$
[1]	CDC report (cumulative cases)	2	2	2	2	2	2	2
[2]	Infected case 1§							
[3]	Infected case 2§							
[4]	Infected case 3§							
[5]	Number of infectives: I_t^\dagger	2	2	2	1	0	0	0
[6]	Number of individuals exiting the infective compartment \ddagger	0	0	0	1	1	0	0
[7]	Number of newly infected individuals	2	0	0	0	0	0	0
[8]	Change in number of infectives from $t-1$ to t : dI_t/dt	2	0	0	-1	-1	0	0

§: Shaded cells indicate the infectious period for each infected case.

†: I_t counts the number of shaded cells for each column t .

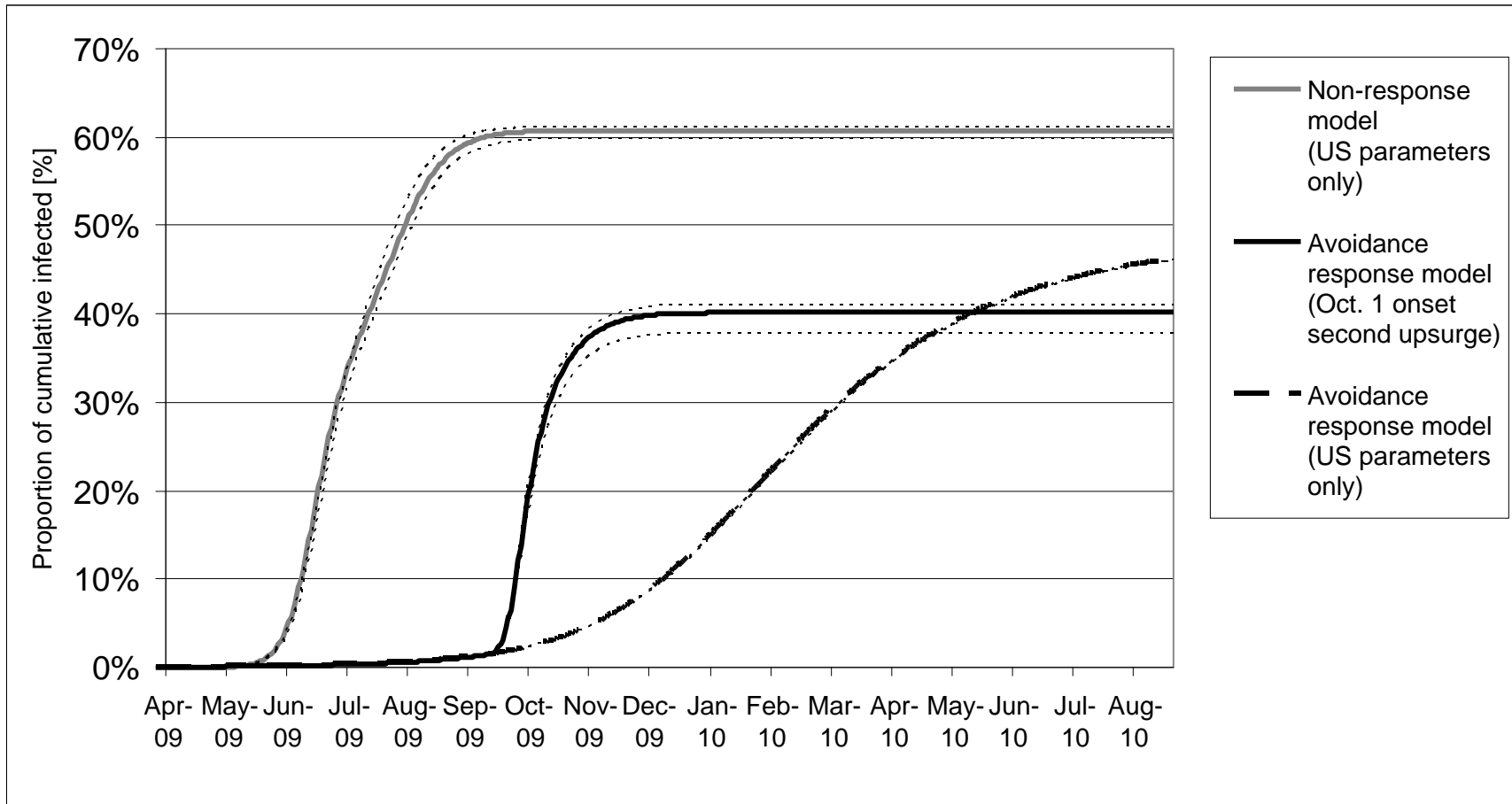
‡: Including deaths due to novel influenza infection (αI_t).

Figure 1. Cumulative confirmed novel H1N1 influenza infected cases in the United States from April 23 to August 31, 2009 (day 86): Real data (up to July 17, 2009) and forecasts by primary avoidance response model and secondary non-response model (95% CI of forecasts by both models are indicated by dashed lines)



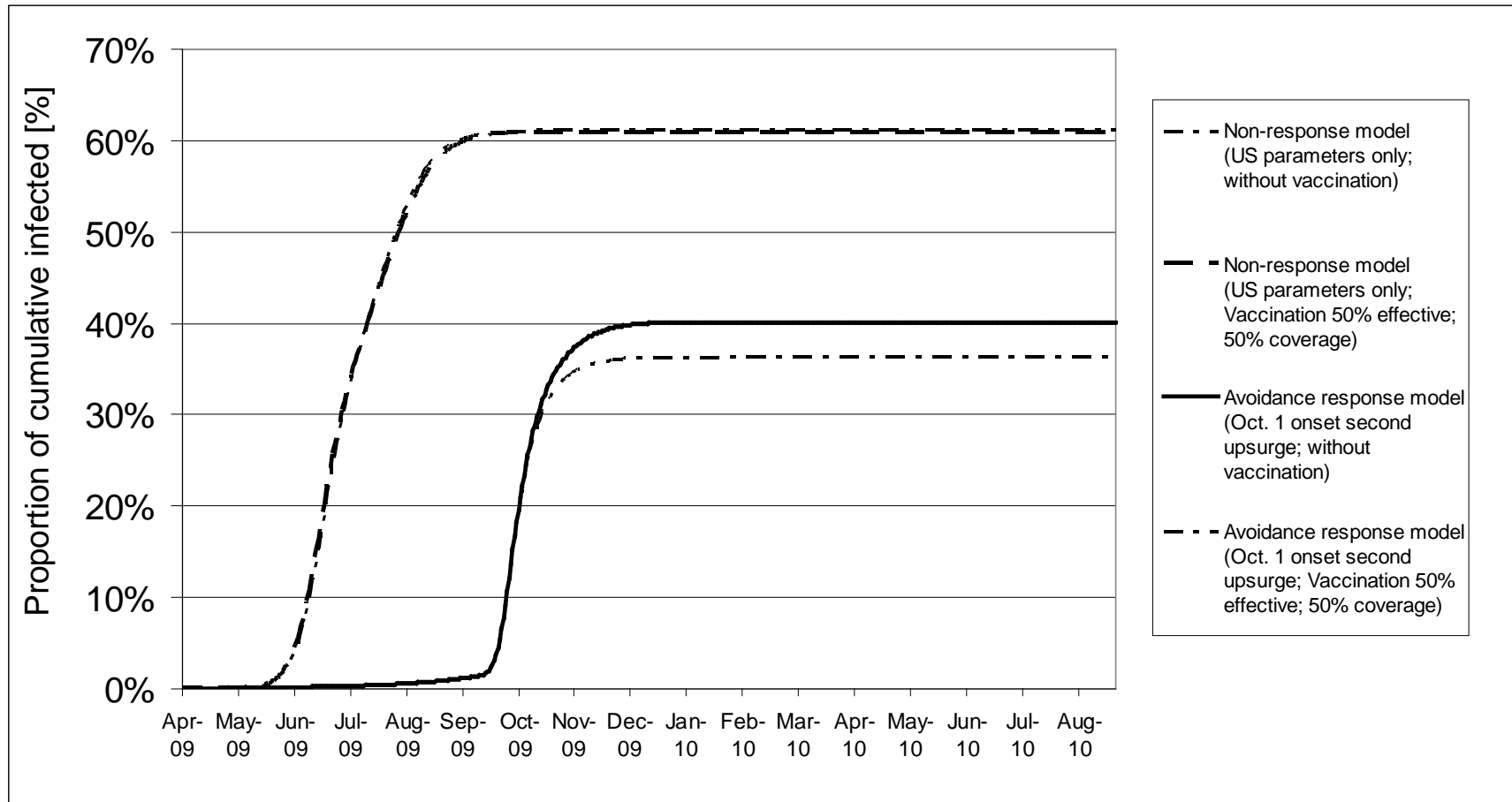
CI represents confidence interval; Non-response model assumed there was no avoidance response. ; Non-response model assumed illness attack rates are 0.343 and .418, which are estimated by the microsimulation among 10 states and 40 states respectively, detailed in the text. Extended forecasts of epidemic paths up to September 2010 of these models are presented in Figure 2 in a different unit [proportion of cumulative infected among total population (%)]

Figure 2. Forecasted novel H1N1 influenza pandemic path measured by [proportion of cumulative infected among total population (%)] in the United States from April 23, 2009 to September 5, 2010 (day 500): 3 scenarios with different assumptions. (95% CI: dashed lines)



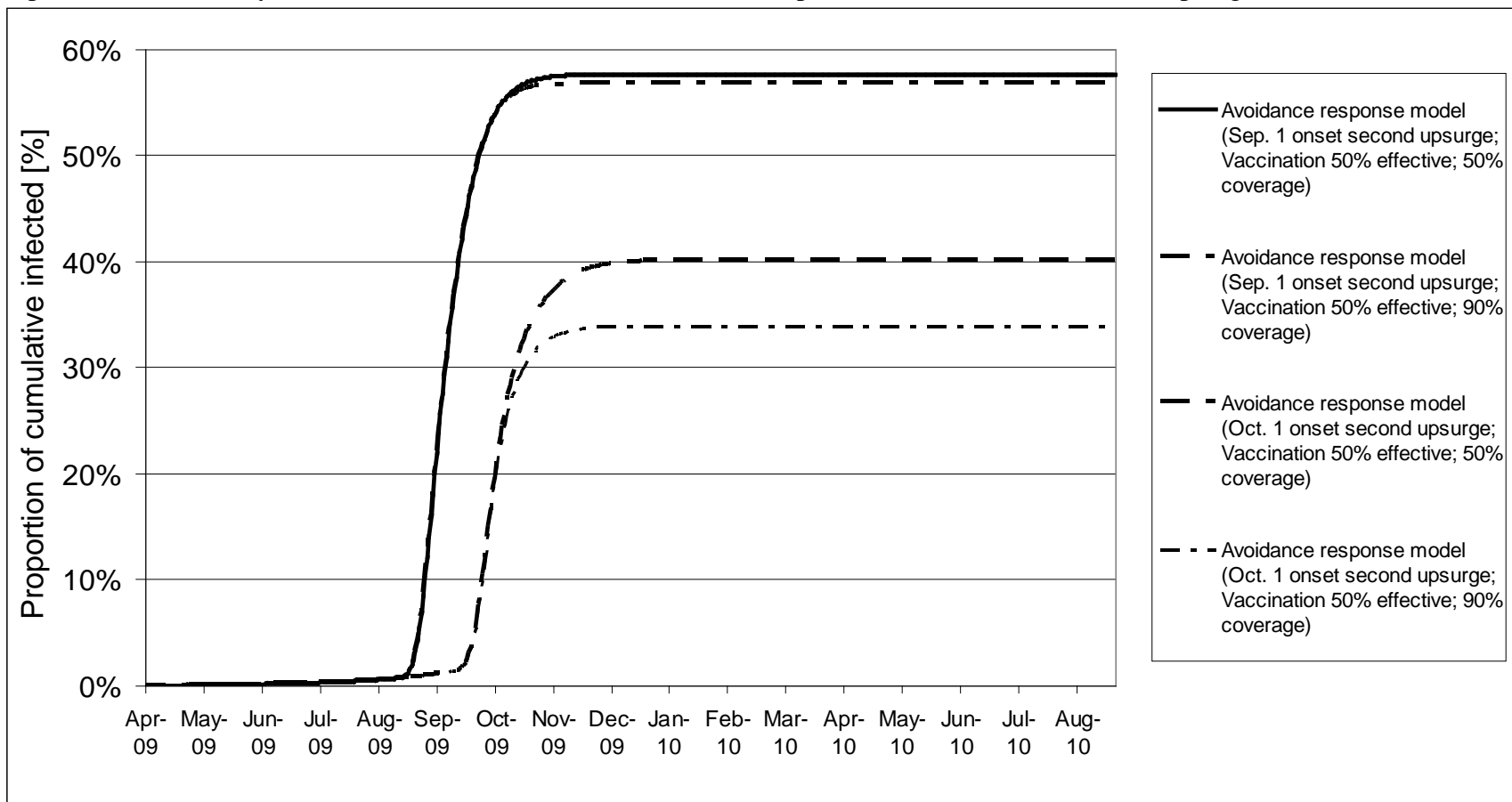
CI represents confidence interval; Non-response model assumed there was no avoidance response; At the onset of a second upsurge, the illness attack rate increased to 0.68. These illness attack rate (0.68) was estimated with the past Australian “winter” data from April to September 2009, detailed in the text.

Figure 3. Forecasted novel H1N1 influenza pandemic path with conservative assumptions about vaccination programs (50% effectiveness and 50% uptake level) measured by [proportion of cumulative infected among total population (%)] in the United States from April 23, 2009 to September 5, 2010 (day 500).



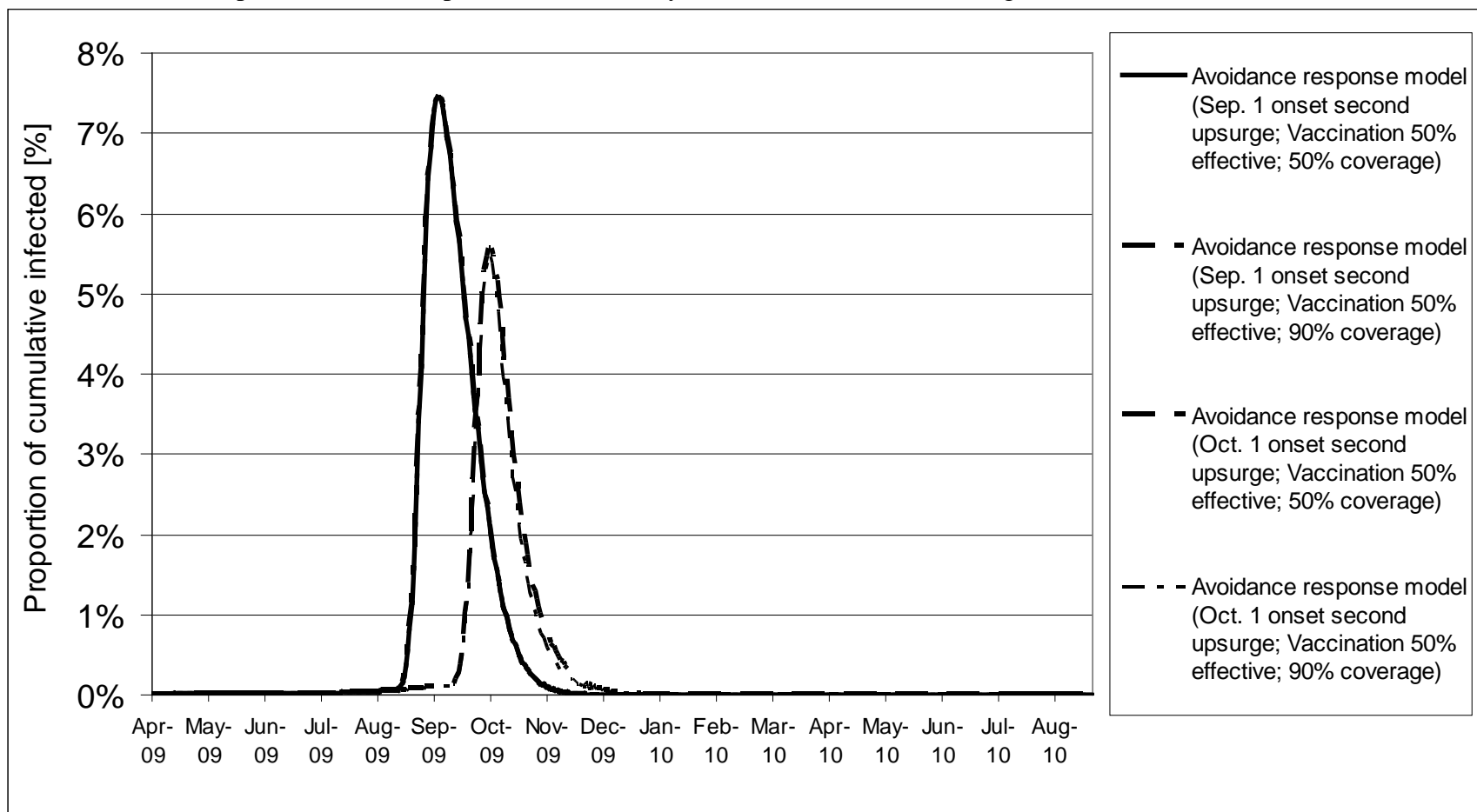
Non-response model assumed there was no avoidance response; At the onset of a second upsurge, the illness attack rate increased to 0.68. These illness attack rate (0.68) was estimated with the past Australian “winter” data from April to September 2009, detailed in the text. Vaccination 50% effective in reducing infection, severe illness and death due to novel influenza. Vaccine coverage rate among the available vaccine doses (October 1-7: 1 million doses per day; October 8-14: 6 million doses per day; October 15- December 2 (7 weeks): 3 million doses per day; 196 million doses in total).

Figure 4. Forecasted novel H1N1 influenza pandemic path with conservative assumptions about vaccination programs (50% effectiveness and 50% uptake level) measured by [proportion of cumulative infected (%)] in the United States from April 23, 2009 to September 5, 2010 (day 500): 4 scenarios with different vaccination uptake rates and different second upsurge onset.



At the onset of a second upsurge, the illness attack rate increased to 0.68. These illness attack rate (0.68) was estimated with the past Australian “winter” data from April to September 2009, detailed in the text. Vaccination is 50% effective in reducing infection, severe illness and death due to novel influenza. Vaccine coverage rate among the available vaccine doses (October 1-7: 1 million doses per day; October 8-14: 6 million doses per day; October 15- December 2 (7 weeks): 3 million doses per day; 196 million doses in total).

Figure 5. Forecasted vaccination benefit in changing the novel H1N1 influenza pandemic peak [prevalence rate (%) and timing] in the United States from April 23, 2009 to September 5, 2010 (day 500): 4 scenarios same as Figure 4.



At the onset of a second upsurge, the illness attack rate increased to 0.68. These illness attack rate (0.68) was estimated with the past Australian “winter” data from April to September 2009, detailed in the text. Vaccination is 50% effective in reducing infection, severe illness and death due to novel influenza. Vaccine coverage rate among the available vaccine doses (October 1-7: 1 million doses per day; October 8-14: 6 million doses per day; October 15- December 2 (7 weeks): 3 million doses per day; 196 million doses in total)